

Review

Metal-Organic Framework-Based Stimuli-Responsive Polymers

Menglian Wei ^{1,*}, Yu Wan ² and Xueji Zhang ¹

¹ Key Laboratory of Optoelectronic Devices and Systems, College of Physics and Optoelectronic Engineering, Shenzhen University, Shenzhen 518060, China; zhangxueji@szu.edu.cn

² Department of Chemistry, University of Alberta, Edmonton, AB T6G 2G2, Canada; ywan3@ualberta.ca

* Correspondence: menglian@szu.edu.cn

Abstract: Metal-organic framework (MOF) based stimuli-responsive polymers (coordination polymers) exhibit reversible phase-transition behavior and demonstrate attractive properties that are capable of altering physical and/or chemical properties upon exposure to external stimuli, including pH, temperature, ions, etc., in a dynamic fashion. Thus, their conformational change can be imitated by the adsorption/desorption of target analytes (guest molecules), temperature or pressure changes, and electromagnetic field manipulation. MOF-based stimuli responsive polymers have received great attention due to their advanced optical properties and variety of applications. Herein, we summarized some recent progress on MOF-based stimuli-responsive polymers (SRPs) classified by physical and chemical responsiveness, including temperature, pressure, electricity, pH, metal ions, gases, alcohol and multi-targets.

Keywords: coordination interaction; stimuli-responsive polymer; sensing



Citation: Wei, M.; Wan, Y.; Zhang, X. Metal-Organic Framework-Based Stimuli-Responsive Polymers. *J. Compos. Sci.* **2021**, *5*, 101. <https://doi.org/10.3390/jcs5040101>

Academic Editor:
Francesco Tornabene

Received: 2 March 2021

Accepted: 29 March 2021

Published: 7 April 2021

Publisher's Note: MDPI stays neutral with regard to jurisdictional claims in published maps and institutional affiliations.



Copyright: © 2021 by the authors. Licensee MDPI, Basel, Switzerland. This article is an open access article distributed under the terms and conditions of the Creative Commons Attribution (CC BY) license (<https://creativecommons.org/licenses/by/4.0/>).

1. Introduction

Mother Nature has served as a great source of inspiration for the design and development of intelligent materials. For example, the sunflower turns toward the direction of sunlight, the Venus flytrap clamps immediately upon the touching of prey, and cephalopods change their body pattern for camouflage [1]. Living creatures change their structures or behaviors adaptively according to the surrounding environment. Thus, by mimicking nature, stimuli-responsive polymers (SRPs) are capable of adapting their physical or chemical properties upon exposure to external stimuli, such as pH, temperature, electromagnetic field, humidity, analytes gradients, etc. [2]. SRPs have attracted significant attention in the scientific community due to their novel properties and show wide applications, such as sensing and biosensing [3], on demand drug or gene delivery [4], actuators [5], catalysts [6], smart coatings [7], disease diagnoses and therapy [8], tissue engineering [9], etc.

One category of SRPs is coordination polymer, namely metal-organic framework (MOF), that is formed by the linkage of metal entities and organic and inorganic ligands [10]. Different from conventional stimuli responsive polymers in which the repeating unit (monomer) is connected through a covalent bond, MOF-based SRPs are constructed via weak interactions, such as metal coordination, hydrophobic association, electrostatic interactions, van der Waals forces, etc. They have been widely used in sensing applications due to their advanced optical properties, such as the intrinsic luminescent feature of sharp emission within a wide spectra range, long luminescence lifetime and large Stokes shift [11–13]. In addition, the features of flexible organic bonds, variable coordination number/geometry and relatively weak metal-ligand interactions in MOFs make them great candidates for sensing as their structure (or conformation) can be dynamically tuned by target analytes [10].

In this review, we focused on the recent progress of MOF-based SRPs toward different stimuli. First, the response mechanism/principles of MOF-based SRPs will be firstly given, followed by a series of examples of MOFs in sensing applications. These examples

were classified into three categories, including physical, chemical and multi-responsive SRPs. Specifically, physically responsive MOFs would change their properties according to temperature, mechanical force and electricity. Chemically responsive MOFs, namely, would show responses to analytes, such as metal ions, anions, explosives, pH, gases, etc. The last category of MOFs is SRPs capable of altering their properties under multiple stimuli. In addition, there are other comprehensive reviews on the topic of MOFs in a different perspective that the readers can refer to [14–24].

2. Sensing Mechanism of MOF-Based SRPs

Generally, four different sensing principles of MOF-based SRP sensors can be classified based on the number of species involved, including metal ions, ligands, auxiliary ligands and guest molecules [16]. The direct approach only involves metal ions and ligands, and the external stimuli impact the coordination environment of the metal ion and ligand, leading to intrinsic optical property changes as shown in Figure 1a. For example, the fluorescence of Zn coordinated 9,10-Bis(pcarboxyphenyl) anthracene (BCPA) MOF was turned off upon the presence of explosives, dinitrotoluene (DNT) and trinitrotoluene (TNT) [25]. The second type works with the addition of auxiliary ligands or metal ions, which compete for the coordination sites in MOFs and play an important part in tuning MOF properties, as shown in Figure 1b. An example was reported by the Mao group that cerium (Ce) coordinated bi-ligands, adenosine triphosphate (ATP) and tris(hydroxymethyl)aminomethane (Tris), Ce-ATP-Tris can serve as artificial peroxidase to detect a low concentration of H_2O_2 selectively due to the fluorescent property switches at different states of Ce(III)/(IV) [26]. Introducing guest molecules improves the selectivity toward specific targets, which are classified to the third cases as shown in Figure 1c. Last but not least, similar to the third case, the presence of guest molecules produces an additional signal along with that from the host, besides improving the selectivity. Thus, the target breaks the host–guest interaction and releases the guest molecules into the environment and produces second signals, which ultimately improves selectivity and reliability.

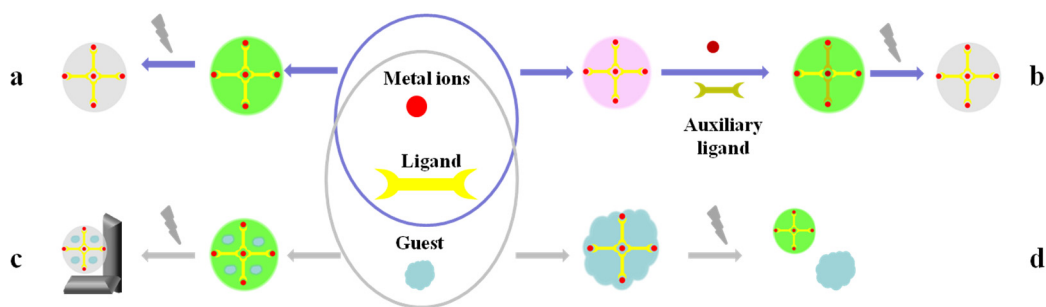


Figure 1. Four different sensing mechanisms of metal-organic framework (MOF)-based stimuli-responsive polymer (SRP) sensors. (a) Direct sensing approach with metal ions and ligand assemblies. (b) Auxiliary ligands or metal ions aided sensing approach. (c) Guest molecules involved sensing approach with improved selectivity. (d) Guest molecules involved sensing approach with dual response signal. Adapted from reference [16]. Copyright 2017, Elsevier.

3. Physically Responsive MOF-Based SRPs

3.1. Temperature Responsive MOFs

Temperature is one of the most important parameters that maintain the physiological process in living creatures. It is also one of the most widely applied external stimuli due to its convenience, noninvasiveness, and remote controllability. Normally, thermally responsive SRPs exhibit lower critical solution temperatures (LCST) or upper critical solution temperatures (UCST), at which phase transition behavior can be observed with increasing or decreasing temperatures, respectively [27]. In MOF-based SRPs, the backbone or side chains of the coordination metal complexes provide alternative strategies for designing temperature responsive materials. The luminescence of transition-metal complexes and

lanthanide based MOFs can be significantly impacted by their microenvironment. Thus, temperature-induced conformational change in MOFs can lead to changes in their optical properties of these complexes. Recently, Huang et al. reported a lanthanide doped Zn (II) based MOF composed of 4,4-oxybis-(benzoate) and 1,3-di(4-pyridyl)propane as a linker ligand and Zn (II) as nodes (MOF1), with the chemical structure shown in Figure 2a [28]. A distorted octahedral coordination was created by one Zn^{2+} with four O atoms from two bidentate COO groups of 4,4-oxybis-(benzoate) and two N groups from two 1,3-di(4-pyridyl)propane. The MOF1 forms a two dimensional (2D)-2D interpenetration structure with a hydrophilic channel created along the crystallographic c axis for hosting Ln^{3+} , especially for Eu^{3+} and Tb^{3+} , as shown in Figure 2b. The MOF1 itself emits blue light (peak center around 430 nm) under 300 nm excitation, of which the emission intensity changes reversely with temperature variation. The doping of Tb^{3+} and Eu^{3+} generates additional characteristic peaks around 545 nm and 616 nm from these lanthanide centers, respectively, as shown in Figure 2c. The Ln^{3+} encapsulated MOF1 showed a broader spectrum color-tuning behavior compared to MOF1 with an additional green and red light emission center. At a lower temperature such as 77 K, the predominant emission center raises from the ligand-based luminescence (430 nm), which decreases dramatically with temperature increasing to 200 K and reaches a plateau as temperature further increases, as shown in Figure 1d. However, the lanthanide-centered emission bands (545 nm and 616 nm) showed totally different behavior that firstly increased when heating up to 150 K, followed by a gentle downturn in the range of 150 to 250 K and a sharper decrease when heating further. The unusual optical properties of Ln-doped MOF1 were ascribed to different reasons that can be divided into three phases: 1. Enhanced energy transfer from the ligands to the lanthanide ions (77 K–150 K); 2. Equilibrium between the energy transfer and nonradiative thermal effect (150 K to 250 K); 3. Thermal activation of the nonradiative energy transfer processes.

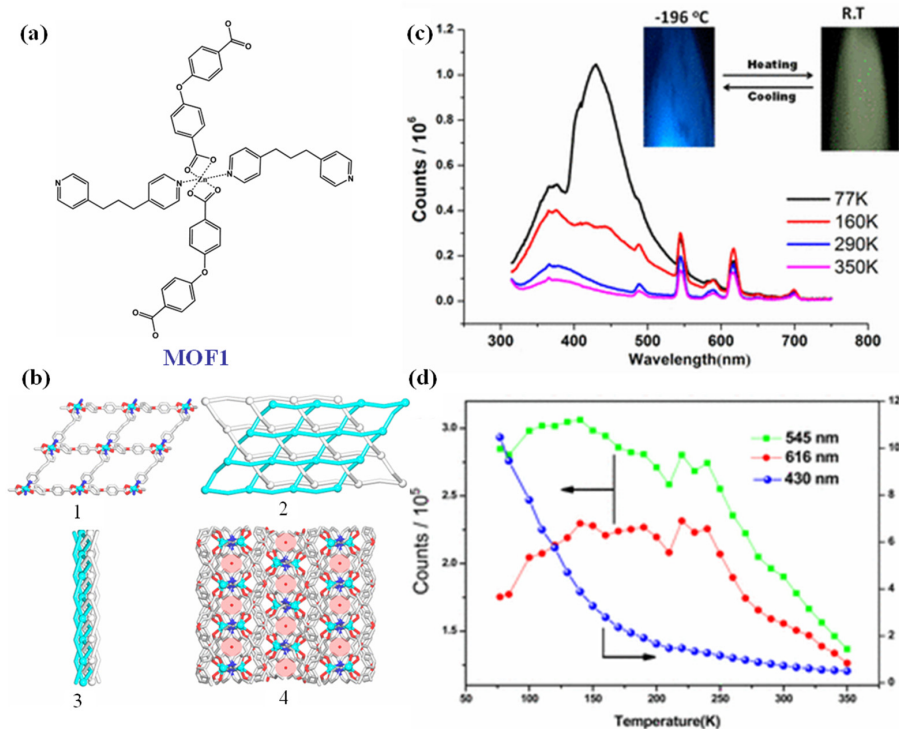


Figure 2. (a) Chemical structure of MOF1. (b) Crystal structure of MOF1 from a different perspective: (1) one layer of 2D MOF1 along b axis; (2) 2D-2D interpenetration of adjacent layer along b axis; (3) 2D-2D interpenetration of adjacent layer along c axis; (4) crystal packing pattern along b axis. (c) Emission spectra of Tb/Eu (molar ratio 47:9) doped MOF1 under 300 nm excitation at different temperatures. (d) Emission intensity change as a function of temperature at various emission centers. Reprinted with permission from Ref. [28]. Copyright 2017, American Society of Chemistry.

A novel self-calibrated and reversible luminescent thermo sensor was reported by Kurup's group which was fabricated by Zn^{2+} metal ions and 2,3-butanedionebisisonicotinylhydrazone as ligand [29]. The Zn (II) based MOF displayed as a 2D-layered structure with the Zn (II) center creates an unusual trigonal prismatic geometry, which is highlighted in brown in Figure 3a. The authors found that the MOF exhibits a reversible yellow to red color change upon temperature switching from 30 °C to 90 °C under UV irradiation. Spectrally, three bands were discovered for this Zn (II) MOF in UV-Vis Kubelka–Munk characterization, including a broad band in the UV region, a second in 350 to 420 nm in the visible region ascribing to intraligand transitions, and a third (above 420 nm) corresponding to charge transfer (CT) transitions. Upon heating, the spectra showed about 50 nm red shift of the CT band while remaining in the same position for the intraligand band. In the photoluminescent (PL) intensity spectra, an emission band around 550 nm was observed with peak red shift as temperature increased. Thus, the authors ascribed the thermochromic behavior of Zn (II) coordination polymer to the desorption process of associated water molecules with concomitant elongation of the Zn–N bond and the disruption of the Zn^{2+} crystal field. Interestingly, the PL intensity of the Zn (II) MOF decreased with elevating temperatures, which is a result of non-radiative relaxation as the loosely packed molecular structure of water molecules is removed. Furthermore, such a thermochromic sensor can be used in document security as shown in Figure 3c, which exhibits vivid colorimetric conversion with heating cycles. Encrypted with the thermochromic Zn (II) MOF, the patterned security feature of “2019” could be readily visualized by applying heat. Such superficial temperature-dependent imaging makes thermal-stimulated writing and tracing possible, which can be potentially used in confidential and reusable purposes.

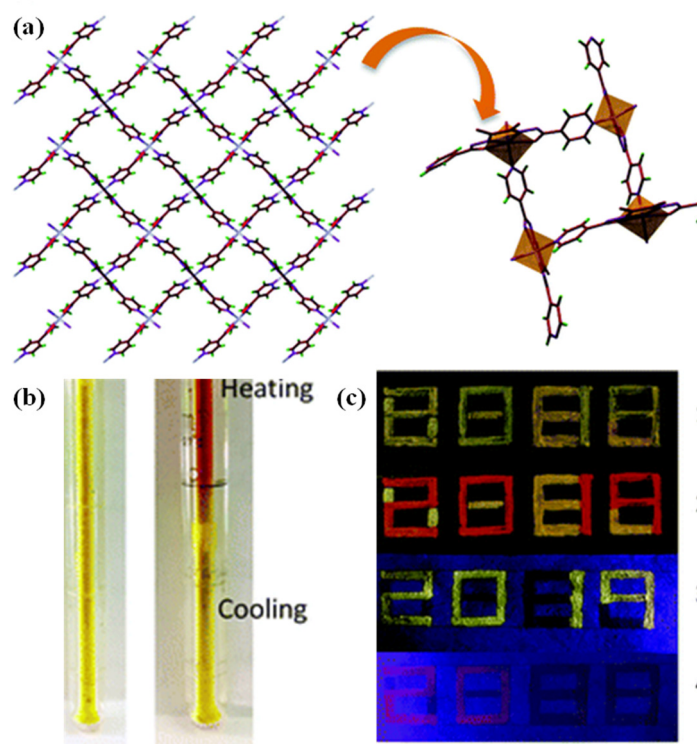


Figure 3. (a) 2D stick view of Zn (II) coordination polymer; zoom in view on the right with the Zn centers highlighted in brown polyhedral. (b) Photos of Zn (II) coordination color change upon temperature gradient. (c) Temperature dependent fluorescence color change for security application; (1) represents the compound at ambient temperatures (2) under 80 °C. A non-thermochromic compound showed temperature stabilization: (3) under UV irradiation and (4) under UV irradiation at 80 °C. Reprinted with permission from Ref. [29]. Copyright 2020, Royal Society of Chemistry.

3.2. Mechanical Force Responsive MOFs

Mechanical force responsive (MFR) materials generally exhibit phase transitions and concomitant property changes upon the application of external force [30]. These materials have been widely used in emerging applications such as wearable electronics [31], tissue engineering [32] and self-healing coatings [33]. Materials with such behavior have been reported in Au nanoribbons [34], perovskite [35], silicon [36], and MOFs [37,38]. Specially, MOF-based MFR materials normally involve crystalline structure re-arrangement or geometry adaption by the introduction of pressure [39]. In some cases, the phase transitions were fully reversible as the external stimuli were removed.

Recently, Cd (II) coordination polymers with formula $[\text{Cd}(\text{L})(\text{DMF})(\text{H}_2\text{O})_2] \cdot \text{H}_2\text{O}$ ($\text{H}_2\text{L} = 5$ -[(anthracen-9-ylmethyl)-amino]-isophthalic acid) (MOF2) were reported by Yan et al. that emit yellowish-green to bright cyan color under UV irradiation as the grinding size decreases [40]. Different from most of the MOF-based MFR polymers, which lose their original crystalline structure under high pressure, MOF2 restores its long range structure with short range structure deformation upon grinding. The mechanoresponsive luminescence of MOF2 arises from the destruction of end-to-face π -stacked arrangements in local defective areas, which suppresses excimer emissions and liberates the ligand-centered emission in the ground sample. Thus, smaller crystal size was generated by a stronger grinding degree, resulting in larger defected areas and more changes of π -stacked interactions. The UV-Vis absorption peaks of MOF2 were gradually blue-shifted as the crystal size decreased, implying that the intermolecular interactions were perturbed by grinding. Similar behavior was discovered in a compound with a chemical component of $[\text{Cd}(\text{INI})(\text{DMF})_2 \cdot \text{DMF}]$ ($\text{H}_2\text{INI} = \text{N}$ -(5-isophthalic acid)-1,8-naphthalimide), with its color changing from weak blue-green to bright blue upon grinding.

The Kodrin group reported a series of mechanically responsive coordination polymers with controllable elasticity by tuning the compositions of ligands [41]. Cadmium(II) halides (Cl, Br, I) were employed as the building blocks of the “spine” that create 1D coordination polymers through bridging halide ions. By the interlinking of directional and relatively weak intermolecular interactions from other 2-halopyrazine ligands, a 2D elastically responsive material was engineered with its long range crystal structure retained as bending, as shown in Figure 4g,h. $[\text{CdX}_2\text{Y}_2]$ ($\text{X} = \text{Cl}/\text{Br}/\text{I}$, $\text{Y} = 2$ -halopyrazine Cl/Br/I-pz) with the combination of ($\text{X} = \text{Br}, \text{Y} = \text{Br-pz}$), ($\text{X} = \text{Cl}, \text{Y} = \text{Cl-pz}$) and ($\text{X} = \text{Br}, \text{Y} = \text{Cl-pz}$) showed relative high elasticity compared to iodopyrazine-based compounds ($\text{Y} = \text{I-pz}$), which can be ascribed to the intermolecular interactions as well as distance difference in the plane perpendicular to the direction of the elongation of the crystal. All of the crystals can be bent easily without fracture and recovered to their original shape immediately upon the removal of the applied mechanical force. The example of a needle shape crystal with chemical component $[\text{CdBr}_2(\text{Br-pz})_2]_n$ is shown in Figure 4a–c. The bending process is repeatable for many times as long as the bending is not beyond the “critical radius”, as shown in Figure 4d–f. In this mechanoresponsive MOF, the halogen-bond/hydrogen-bond interactions between the 2-halopyrazine planes play an important role in maintaining elasticity.

The Maurin group have reported that serials of MOFs show mechanical responsiveness that exhibits volume phase transition via applying external pressure [42–44]. For example, a 14% volume change with irreversible structural change was observed in dehydrated gallium fumarate MOF, donated as MIL-53(Ga)-FA, upon applying pressure of 85 MPa, which could potentially be applied as mechanical energy storage [42]. Similarly, by switching the metal center from Ga to aluminum (Al), dehydrated MIL-53(Al)-FA demonstrated structural contraction when the applied pressure is above 100 MPa [44]. Interestingly, such a deformation is fully reversible in the compression–decompression cycles with the presence of a hysteresis of about 125 MPa compared to MIL-53(Ga)-FA.

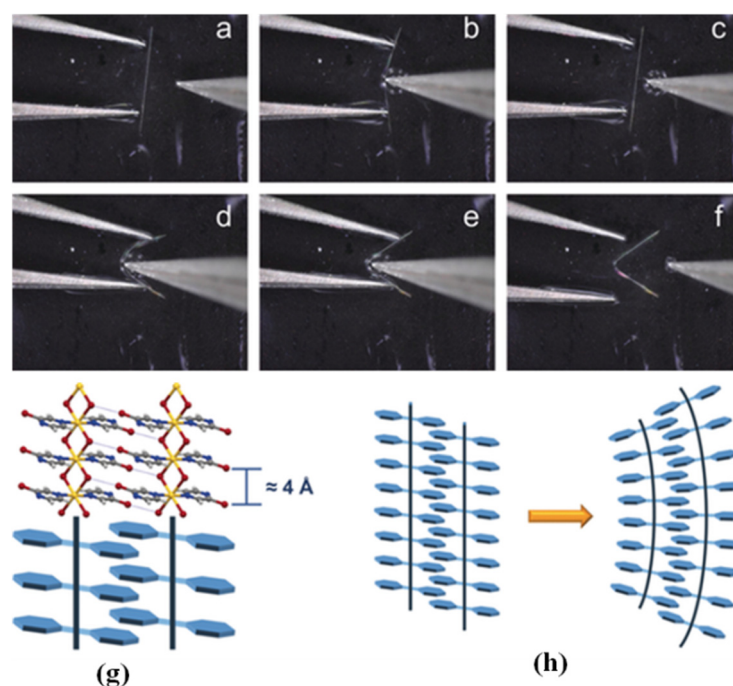


Figure 4. Snapshots of repeated elastic bending motion (a–c) of a needle-shaped crystal of $[\text{CdBr}_2(\text{Brpz})_2]_n$. The crystal breaks when it is bent beyond a critical radius (d–f). Bending was performed by a pair of tweezers and a needle. (g) Crystallographic illustration of Cd (II) coordination polymer with Cd halides as spine and interlinked by 2-halopyrazine. (h) Structural model as elastic bending with long range crystal structure retained. Reprinted with permission from Ref. [41]. Copyright 2018, Wiley-VCH Verlag GmbH and Co. KGaA.

3.3. Electrically Responsive MOFs

Electrically responsive polymers normally exhibit phase or volume transition under the electric stimuli. The incorporation of redox sensitive units, such as disulfide bond [45], viologen [46], ferrocene [47], benzoquin [48], etc., plays an important role in successfully fabricating electrically responsive materials. For example, the valence state of iron ions in ferrocene can be dynamically changed by a redox reaction, which ultimately impacts the intermolecular interactions (host-guest interactions or/and hydrophilic/hydrophobic) in a complex. Nakahata et al. reported supramolecular materials using cyclodextrins modified with poly(acrylic acid) (pAA-CDs) as a host polymer and pAA processing with ferrocene (pAA-Fc) as a guest polymer, of which the sol-gel phase transition can be dynamically tuned by either the addition of oxidization/reduction species (NaClO/glutathione) or applying voltages [49]. Wang's group also showed that the binding affinity between per-butylated pillar [6] arene and ferrocene decreased significantly as the ferrocenium cations reduced to ferrocene [50]. All these examples demonstrate feasible approaches for electrochemically controllable functional materials with redox-responsiveness.

Ghoufi et al. have reported a series of chromium(III) dicarboxylate (MIL-53) with a chemical formula of $\text{Cr}(\text{OH}) \cdot \{\text{O}_2\text{C}-\text{C}_6\text{H}_4-\text{CO}_2\} \cdot \{\text{HO}_2\text{C}-\text{C}_6\text{H}_4-\text{CO}_2\text{H}\}_x \cdot \text{H}_2\text{O}_y$, which exhibit an interesting breathing effect that the open pore closed upon guest adsorption and reopened again at saturation load [51]. The similar behavior of pore closing was observed at an applied field strength of about 1.75 GV/m, while it reopened in a hysteresis fashion as the field strength decreased. By dynamically tuning the pore size with the electric field, the authors showed the selective separation over carbon dioxide and methane, which demonstrates the possibility to tune adsorption properties by the electric field.

Along with volume phase transition in electrically responsive MOFs, other properties such as conductivity can also be impacted by the external electric field. Recently, Fernandez et al. reported an electrically switchable MOF composed of $\text{Cu}(\text{TCNQ})$ ($\text{TCNQ} = 7,7,8,8-$

tetracyanoquinodimethane) that exhibits a reversible high-resistance to conducting state transitions by an applied potential [52]. Two polymorphs of Cu(TCNQ) can be synthesized at different temperatures or reaction times, as shown in Figure 5a,b. Phase I is a highly distorted tetrahedron with the neighboring TCNQ molecules perpendicular to each other. In contrast, the TCNQ molecules in phase II are coplanar and oriented in the same direction but in two perpendicular planes. Phase I demonstrated several orders of magnitude higher conductivity than phase II, which can be attributed to the π -stacking created by adjacent TCNQ molecules interpenetrating in phase I and the interactions between the metal's d orbitals and cyano's p orbitals. Upon applying external voltages in the range of 2.5 V to 5 V, the authors proposed that a third phase exists with the investigation of X-ray diffraction (XRD) techniques, as shown in Figure 5c. Thus, the applied potential leads to the distortion of tetrahedral symmetry at the Cu positions and concomitant overlap of the hybrid sp orbitals of the cyanide functionalities and the π system of the benzene rings, which was revealed as conductivity increased. A further increase in applied potential to 6 V would lead to transition from phase III to phase I, involving bond breakage, framework rearrangement and the formation of new Cu-N coordination bonds, which were not observed at 3 V or 5 V. The higher potential applied provided enough energy for bond breakage and formation.

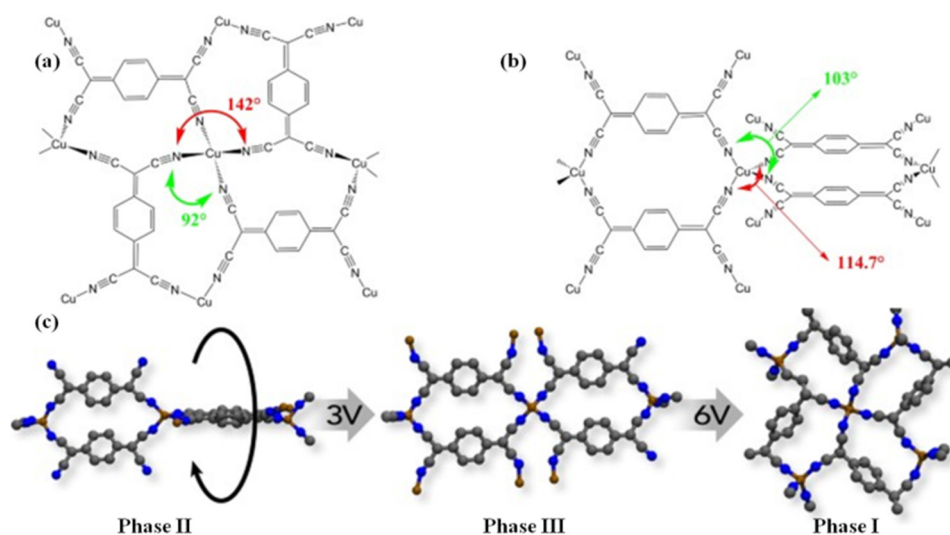


Figure 5. Chemical structure of Cu(TCNQ) in phase I (a) and phase II (b). (c) Single crystal structure transition of Cu(TCNQ) from high resistance state (phase II) to proposed new state at 3 V (phase III) followed by transition to conductive state (phase I) at 6 V. Reprinted with permission from Ref. [52]. Copyright 2014, Nature Publishing Group.

Electrochromic materials are capable of reversible color change when external electric stimuli are applied [53]. It is commonly observed in π -conjugated polymers as of the reversible transition between several redox states. The diverse redox properties of electrically responsive MOFs allow them to serve as multicolored electrochromic materials, and they have been widely used in electronic display devices. Viologens (V^{2+}), 4,4'-Bipyridinium salts, are well-known electrochromic materials that exhibit three reversible redox states, namely, V^{2+} (dication, pale yellow colored/colorless), V^+ (radical cation, violet/blue/green) and V^0 (neutral, colorless). Kahlfuss et al. recently reported a viologen-hinge based supramolecular system coordinated by palladium, which can undergo a fold to stretch conformation transition under electric stimulation [46], as shown in Figure 6. The short and flexible propylene link was used to connect two viologen units. The molecule exhibits as extended state due to the strong repulsion between dicationic viologen units. However, it undergoes an extension-to-fold conformational transition due to the reduction of V^{2+} to V^+ . The electrically triggered folding motion was driven by the π -dimerization of the electro generated viologen cation radicals. The palladium ions are capable of binding to the ditopic ligand in both folded and elongated state as the

planar features and small triazole/pyridine-containing binding sites. A 1D self-assembled structure can form as the coordination between Pd^{2+} and ditopic redox-responsive tecton, which exhibits large scale architecture reorganizations (sol-gel transition) in solution upon electric stimulation.

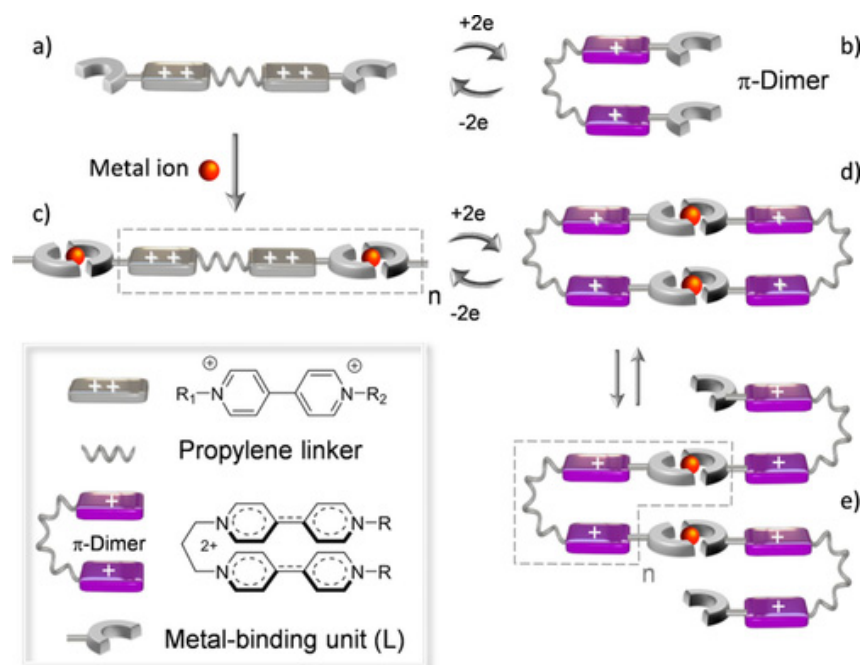


Figure 6. Schematic illustration of electrochemically driven reversible extension to folding conformational change in the absence (a,b) and in the presence (c–e) of metal ion. Two possible folding structures (d,e) were available in the association and/or the organization of tectons within metal-ligand assemblies upon the electric stimuli. Reprinted with permission from Ref. [46]. Copyright 2018, Wiley-VCH Verlag GmbH and Co. KGaA.

4. Chemically Responsive MOF-Based SRPs

4.1. pH Responsive MOFs

pH responsive polymers usually contain proton donating or accepting groups in their monomers, which may affect the solubility or gelation process [54]. Proteins are one of the most well-known examples that have carboxylic acid and amine groups coexisting and are capable of precipitation as the environmental pH changes. The pH sensitive MOFs can be generated by incorporating proton donating/accepting groups in a coordination structure, which can be potentially used in a drug delivery system due to the acidic environment of the tumor cell. Recently, Gao et al. reported Fe^{2+} and 1,1'-(1,4-butanediyl)bis(imidazole) (bbi) based coordination polymer spheres as anticancer drug carriers for pH triggered drug delivery [55]. The nanoscale coordination polymer sphere was synthesized by coordination polymerization followed by a fast precipitation with a thin layer of silica coating on the surface preventing it from rapid dissolution. As the protons can bind to the organic ligand bbi competitively, the stability of the coordination structure of Fe^{2+} and bbi can be interrupted by the surrounding pH changes, leading to the anticancer drug releasing in an acidic environment. In addition, the conjugation of folic acid on the coordination nanosphere improved the selectivity in cancer cell targeting.

Ma et al. reported two new pH sensitive benzothiadiazole-derived coordination complexes with formulas of $[\text{Zn}_{0.5}(\text{TBC})(\text{H}_2\text{O})]$ (TBC = 4-cyano-7-(1H-tetrazol-5-yl)benzothiadiazole) and $[\text{Cd}(\text{TBC})(\text{N}_3)(\text{H}_2\text{O})]_n$, which were synthesized by click reaction in hydrothermal conditions [56]. The authors showed that the Zn-based MOF self-assembled into a 3D supermolecular structure via intermolecular hydrogen bonds and N–S interactions, as shown in Figure 7a. In detail, the Zn (II) ion was symmetrically chelated by two deprotonatedly

planar TBC ligands in a trans configuration. An octahedral geometry was formed around the Zn (II) center by two benzothiazole (BTD) nitrogen atoms, two tetrazole nitrogen atoms, and two water oxygen atoms. In the case of a Cd-based MOF, it is composed of undulated 2D layers with a $(8)(8^4 \bullet 12^2)$ topological network, as shown in Figure 7b. The adjacent layers were stacked into a 3D supramolecular structure via interlayer N–S interactions. Both BTD-derived complexes exhibit fluorescent emission under UV irradiation, with an emission center (570 nm) for the Zn-based MOF and two emission centers (490 and 568 nm) for the Cd-based MOF. The authors ascribed this to the different decay procedures of the $\pi \rightarrow \pi^*$ states of BTD species. The fluorescent emission of the Zn (II)-based MOF is quenched in an acidic environment, while it is recovered in a neutral environment due to the protonation enhanced electron-withdrawing nature of the tetrazole group. On the other hand, the Cd-based MOF exhibited the self-referencing fluorescence response in an alkaline environment as of the different proton-withdrawing capability of the coordinated tetrazole group.

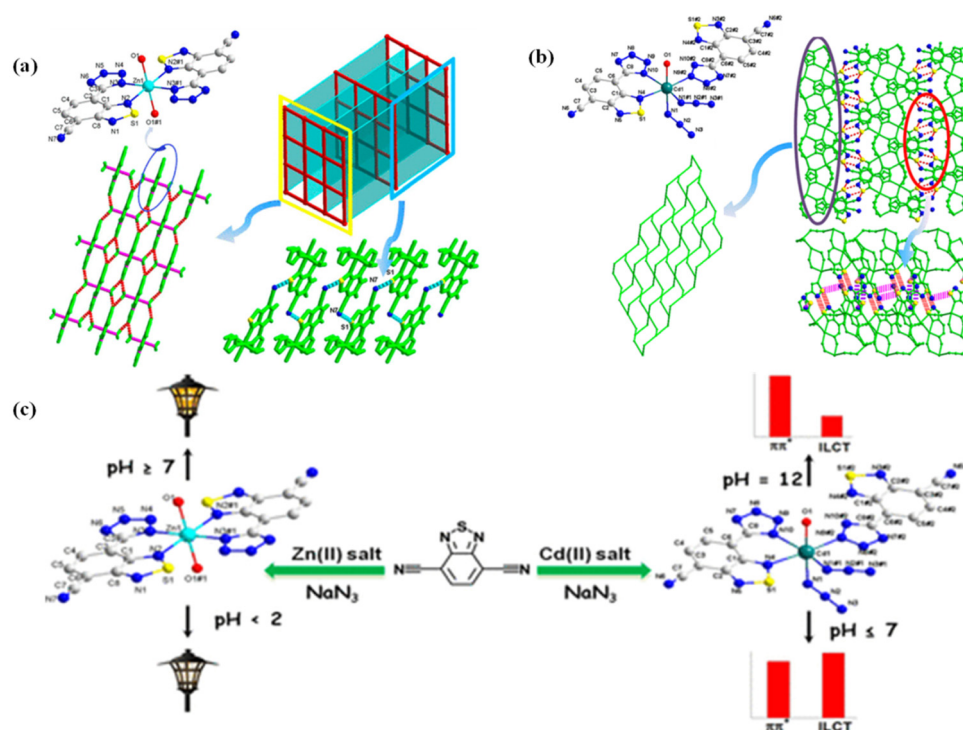


Figure 7. (a) Schematic illustration of Zn (II)-based MOF in monomeric structure and 3D supramolecular coordination with 4^4 -subnets by hydrogen bonding (2D 4^4 -subnet layer formed by hydrogen bonding, red dotted line) and interlayer N–S interactions (light blue dotted line) (all the hydrogen atoms are omitted for clarity). (b) Schematic illustration of Cd (II) coordination environment and its 3D supramolecular network as of the undulated 2D $(8)(8^4 \bullet 12^2)$ -subnets by interlayer N–S interactions (red and magenta dotted line) (all the hydrogen atoms are omitted for clarity). (c) Illustration of pH responsiveness of Zn and Cd-based MOF. Reprinted with permission from Ref. [56]. Copyright 2018, American Society of Chemistry.

Another pH dependent photoluminescent MOF was reported by Yan et al. with a chemical formula of $[ML(H_2O)]_n$ (M: Zn and Co, H_2L : 4-(2-chloroimidazo[1,2-a]pyridine-3-carboxamido) phthalic acid) in a one-dimensional (1D) ladder-like chain structure [57]. The adjacent ladder chains were linked by hydrogen bonds and lone-pair- π interactions. The carboxylate anion (COO^-) in these complexes can be protonated into carboxylic acid ($-COOH$) upon exposure to HCl vapor. Thus, interest reversible luminescent switching behaviors were observed in these systems upon the acid-base vapor stimuli due to the protonation-deprotonation processes mediating the lone-pair- π and cation- π interaction conversion. The Zn-based MOF reveals a blue-shifted emission as of ligand-to-metal

charge transfer, while the Co-based MOF presents a dominant antiferromagnetism. Such switchable behavior in response to external HCl and NH₃ vapor stimuli might be of great importance for practical application in optical recording, sensing, or molecular device and switch.

Tan et al. reported a terbium-based MOF material Me₂(NH₂)₂[Tb₂(L)₂](H₂O)₆, L = 1-(3,5-dicarboxylatobenzyl)-3,5-pyrazole dicarboxylic acid with good water-stability and strong luminescent emission under UV light excitation [58]. Uric acid can specifically quench the luminescence due to its weak interaction with ligands over many other interferences including urea, creatine, HA (hippuric acid), sucrose, Glu (glutamic acid), K⁺, Na⁺, PO₄³⁻ and HPO₄²⁻. Such behavior was employed for uric acid sensing in aqueous media and showed a limit of detection (LOD) down to 7 nM.

4.2. Metal Ion Responsive MOFs

The lanthanide ion complex exhibits excellent luminescence characteristics, such as sharp emission in the invisible and near IR region, high photoluminescence efficiency and long excited-state lifetime [59]. The strong metal-centered luminescence under appropriate UV irradiation can be ascribed to the so-called “antenna effect” [60], which involves consecutive processes of initial ligand optical absorption, followed by ligand-to-metal energy transfer and lead to metal-ion-based fluorescence. A series of lanthanide coordination polymers (Ln-CPs), {[Ln(HL)(H₂O)₂](H₂O)₂]_n (Ln = Eu, Tb, Gd, Sm, Dy, Nd, Pr, Er) [H₄L = (1,1':3',1''-terphenyl)-3,3'',5,5''-tetracarboxylic acid] was reported by Shi et al. composing a two dimensional network in which dinuclear units are interconnect by dual carboxylate bridges [61]. Among those, Eu and Tb-based Ln-CPs showed great thermal stability up to 400 °C and chemical resistance in acid/base aqueous solutions and different water/ethanol solutions, which make them great candidates as functional materials for sensing ions and explosives. Notably, the Tb-based MOF displayed fast response in 10 s and excellent recyclable behaviors (at least 10 times) for sensing Fe³⁺ and Cr₂O₇²⁻ effectively with an LOD of 0.28 μmol L⁻¹ and 0.36 μmol L⁻¹, respectively. In addition, it shows great selectivity over other cationic (Ba²⁺, Ni²⁺, Co²⁺, Ca²⁺, Mg²⁺, Na⁺, K⁺, Zn²⁺, Mn²⁺, Al³⁺, Cu²⁺, Fe³⁺) and anionic ions (SCN⁻, I⁻, F⁻, ClO₃⁻, IO₃⁻, SO₄²⁻, C₂O₄²⁻, HSO₄⁻, CO₃²⁻). Regarding the sensing mechanism of Fe³⁺, the authors ascribed it to a series of combinational processes of the inner filter effect, weak interaction and electron transfer enhanced the quenching efficiency, which ultimately lowered the limits of both selectivity and sensitivity. In the case of the selective detection of Cr₂O₇²⁻, the inner filter effect is the dominating factor which shows the overlap of excitation of Eu and Tb-based MOFs. Moreover, the ability to detect explosives of Ln-CPs (Eu and Tb) was also studied and found to have great selectivity to p-nitrophenol (4-NP) and trinitrophenol (TNP), which was ascribed to electron transfer and the inner filter effect. Interestingly, trichromatic color tuning including white light emission and linear dependent dichromatic color tuning among red, green and blue primary colors can be achieved by combining two or three Ln³⁺ ions (Eu³⁺, Tb³⁺, Gd³⁺) in metallic compounds.

Guan et al. reported a spongy supramolecular polymer gel (SHG) consisting of naththalimide functionalized-pillar[5]arene as a host and a tripodal guest via multi-non-covalent interactions, with the structure shown in Figure 8 [62]. The SHGs exhibit aggregation induced emission properties that produce yellow fluorescence (520 nm) under UV irradiation, while quenched under exposure to Fe³⁺ ions. This behavior of SHGs can be employed for Fe³⁺ ion sensing with specificity over other metal ions, such as Ba²⁺, Ca²⁺, Zn²⁺, Co²⁺, Ni²⁺, Cu²⁺, Mg²⁺, Hg²⁺, Cd²⁺, Ag⁺, Na⁺, Al³⁺, La³⁺, and Pb²⁺, with an LOD of 0.9 nM. The authors proposed the sensing mechanism as the Fe³⁺ binding to SHG through a cation-π interaction that alters the non-covalent intra-molecular interaction and ultimately leads to SHG structural change and the electron transfer process.

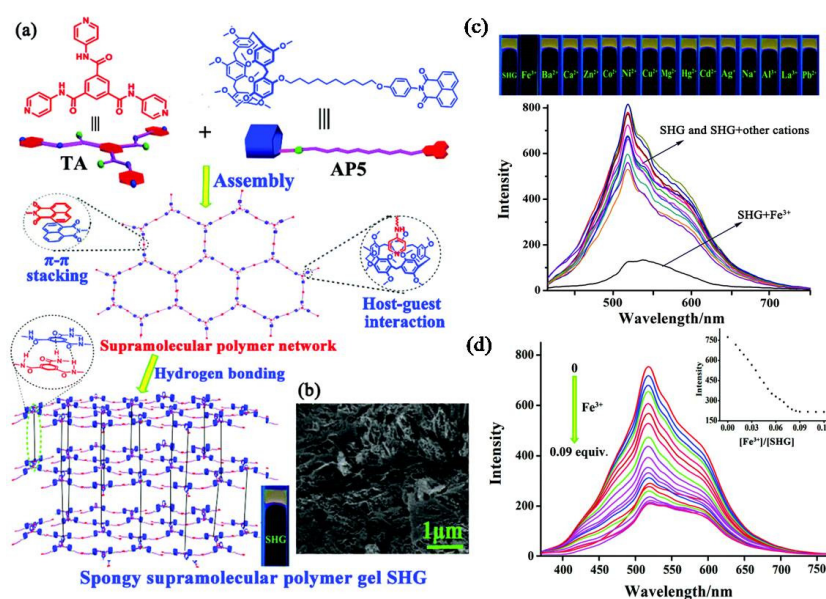


Figure 8. (a) Host and guest molecule chemical structure and proposed assembly mechanism into supramolecular polymer gels (SHGs) (b) SEM images of SHGs. (c) Top: images of SHG and different cations mixture under UV irradiation; bottom: fluorescence spectra of SHG with addition of different cation aqueous solutions. (d) Fluorescence spectra of SHG with increasing concentrations of Fe^{3+} ($\lambda_{\text{ex}} = 280 \text{ nm}$, $\lambda_{\text{em}} = 520 \text{ nm}$). Reprinted with permission from Ref. [62]. Copyright 2019, Royal Society of Chemistry.

The Rowan group has reported a series of metallo-supramolecular polymers in organophosphate sensing based on 2,6-bis(1'-methylbenzimidazolyl) pyridine (Mebip) as the ligand and lanthanide ion (Eu^{3+}) [63,64]. Any analyte that plays as a competitive binder for the Eu^{3+} center can quench Eu^{3+} -based emission and potentially restore the emission of the “free” ligand. By combining other transition metal omission ligands with metal-based emissions such as Zn and La, both mechanical and optical properties (quench or shift) can be tuned on demand.

4.3. Gas Responsive MOFs

The porous structure in MOFs makes them ideal candidates for gas storage and sensing. The selective combination of metal ions and ligands can generate MOFs with tunable size, shape and surface chemistry, which offers the advantages of flexibility in structure over other conventional porous materials [65]. Normally, gas molecule adsorption can induce a closed/open switch of MOF conformational change, which can be applied for selective gas detection.

Chen et al. developed a coordination polymer-based colorimetric sensor for ammonia detection [66]. The polymer is composed of $[\text{Cd}_2(\text{pbpy})(\text{bdc})_2\text{I}_2] \cdot 4\text{H}_2\text{O}$ ($\text{H}_2\text{bdc} = 1,4$ -benzenedicarboxylic acid; $\text{pbpy} \cdot 2\text{ClO}_4^- = 1,1'$ -[1,4-phenylenebis-(methylene)]-bis(4,4'-bipyridinium) perchlorate) that exhibits a rapid white to yellow chromic response upon exposure to ammonia vapor. The weakly coordinated iodine anions were replaced by ammonia molecules, which changed the structure of the coordination polymer and yielded a new charge transfer route.

Yanai et al. recently reported an MOF-based CO_2 sensor by introducing a reporter molecule, distyrylbenzene (DSB), that is capable of giving fluorescent signal change upon the conformation change of the flexible coordination polymer [67]. Due to the adsorbing of the target molecule CO_2 as a second guest, the original host–guest interactions were affected with concurrent size and shape re-arrangement, which ultimately led to reporter conformation change and fluorescent variation, as shown in Figure 9a. The host molecule is composed of $[\text{Zn}_2(\text{terephthalate})_2(\text{triethylenediamine})]_n$ and exhibits as two-dimensional

(2D) square grids that are bridged by triethylenediamine. The guest molecules (DSB) slide in the nanochannels of the host molecules, as shown in Figure 9b. The authors found out that the resultant host–guest complexes can selectively adsorb CO₂ over other atmospheric gases, such as N₂, O₂, and Ar. In addition, gases molecules with similar physicochemical properties to CO₂, such as acetylene (C₂H₂), can also be differentiated by this host–guest complex by means of different luminescence outputs. Taking advantage of the structural flexibility of the MOF, the aforementioned composite system demonstrated the first example of gas detection with fluorescent signal variation in organic molecules without any chemical interaction or energy transfer. The co-operative host–guest-based detection method provided alternative approaches in the development of advanced gas sensing systems.

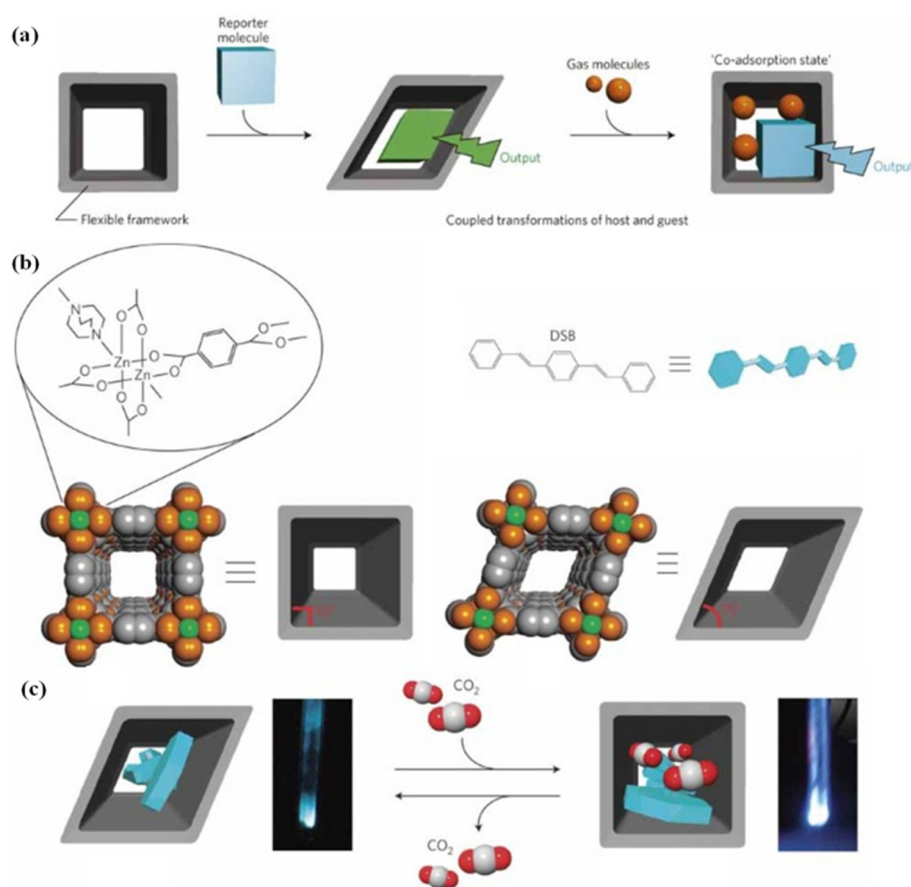


Figure 9. (a) Schematic illustration of gas molecule detection mechanism. By inclusion of a reporter molecule, the flexible coordination polymer framework adapted an induced-fit-type structural change. Upon further gas adsorption, the host–guest structure transformed with pore size variation and conformational variations of the reporter molecule, which leads to a change in output signal. (b) Crystallographic illustration of host molecules (left) with metal ion coordination environment zoomed in. The original (left) and deformed (right) structures of host molecules. Chemical structure and representative diagram of reporter molecule DSB. (c) CO₂ sensing mechanism. Conformation and fluorescent signal change of host–guest molecules upon the introduction of CO₂. The pictures of complexes were taken at 195 K under UV irradiation. The removal of CO₂ was accomplished in vacuum at 195 K. Reprinted with permission from Ref. [67]. Copyright 2011, Nature Publishing Group.

In another example of gas sensing, crown ether-based host–guest interactions with Ag coordination were used to produce hydrogen sulfur sensitive supramolecular polymers, which go through several assembly processes as shown in Figure 10 [68]. In detail, a pseudo[3]rotaxane was firstly formed with benzo-21-crown-7 as the host molecule (H) and a homoditopic guest G via host–guest interaction. To further link pseudo[3]rotaxane,

the Ag(I) ion was introduced due to its coordination towards the pyridyl group in host molecules. However, these coordinations can be interrupted with supramolecular polymer disassembly in the presence of H₂S due to the Ag(I) ions' precipitation. Herein, an H₂S-sensitive supramolecular polymer was constructed with its structure dynamically assembled and disassembled by Ag/H₂S pairs.

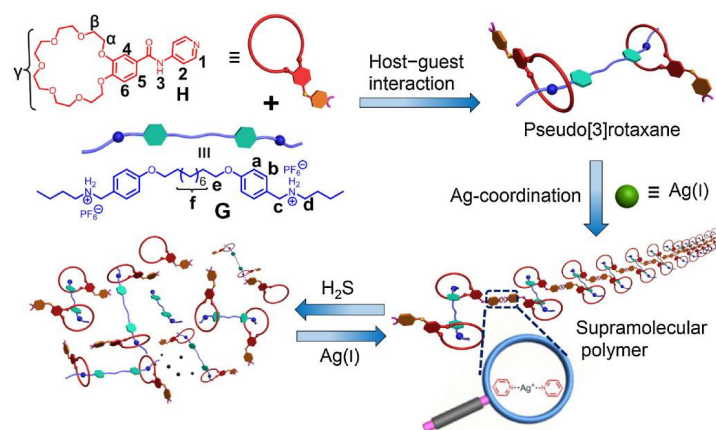


Figure 10. Schematic representation of assembly of supramolecular polymers and its response to H₂S. Pseudo[3]rotaxane was firstly formed with benzo-21-crown-7 as the host molecule (H) and a homoditopic guest G via host–guest interaction. The further addition of Ag ions created supramolecular assemblies due to the coordination interaction between Ag and pyridyl group in H. The assemblies' structural can be dynamically tuned by H₂S. Reprinted with permission from Ref. [68]. Copyright 2019, Elsevier.

Besides the porous structure for gas molecule capture, a HCl vapor sensitive non-porous one-dimensional coordination polymer [Cu(pyim)(Cl)(MeOH)] [1, pyimH = 2-(imidazol-2-yl)pyridine] was recently reported based on chemisorptions with covalent bond cleavages and formation [69]. The crystallinity of the coordination polymer was retained upon the chemisorption process, while it showed profound structural changes with concurrent magnetic property variation. In detail, the pentacoordinated square-pyramidal Cu centered compound 1 changed into ionic form (H₂pyimH)[CuCl₄] (2) with distorted tetrahedral [CuCl₄]²⁻ anions when three equivalent HCl molecules were adsorbed chemically. The single crystal broke into polycrystalline powder with a color change from dark green to yellow in a few minutes. The extruding of two equivalent HCl in ionic compound 2 yielded a square-planar Cu centered cis-[CuCl₂(pyimH)] (3). The sequential structure changes involved remarkable rearrangement of covalent bonds and drastic changes in magnetic properties, from strong antiferromagnetic interactions of 1 to weak ferro- or antiferromagnetic interactions in 2 and 3, respectively. The process of HCl chemisorption led to the protonation of imidazolate ligand and modified the geometry around the Cu centers, which switched off the efficient Cu–Cu exchange pathway.

4.4. Alcohol Responsive MOFs

Alcohol strength (AS), the volume percentage of ethanol at 20 °C, is an important parameter that was monitored in spirit drinks for quality control and regulation. MOF-based strategies have been developed for AS qualification. For example, a lanthanide coordination polymer complex was developed as a ratiometric fluorescence sensor in ethanol percentage monitoring [70]. The supramolecular complex (C343@Eu-TDA) is constructed with metal ions Eu³⁺, ligand 2,2'-thiodiacetic acid (TDA), and a cofactor ligand coumarin 343 (C343). The coordination polymer Eu-TDA itself emits a red fluorescence at 617 nm under UV irradiation. Upon the chelating of cofactor ligand, the red fluorescence was enhanced, with the fluorescence of C343 at 495 nm diminishing due to the energy transfer from C343 to Eu³⁺. The C343@Eu-TDA is stable in pure ethanol, while it disassembled

into Eu-TDA and C343 with the addition of water. The dissociation of C343 from the coordination complex (C343@Eu-TDA) resulted in a red to blue fluorescent change. Thus, the ethanol percentage in the spirit sample can be quantified by monitoring colorimetric variations. The method developed here showed a linear dynamic range of 10% vol to 100% vol in AS quantification of different spirit samples via “naked eye” under UV-lamp (365 nm). In addition, it showed great selectivity over other solvents, such as methanol, ethanol, isopropanol, 1-butanol, 1-hexanol, and 1-octanol. By rationally designing the optical properties of the metal–ligand framework and the cofactor ligand, the method developed here provides alternative approaches for on-the-spot visible AS detection.

A similar approach was reported by using Zn^{2+} as the central metal ion, 1,4-bis(imidazol-1-ylmethyl)benzene (bix) as the ligand, and rhodamine B (RhB) as the cofactor ligand [71]. The supramolecular network is stable in pure ethanol solvent with no fluorescent emission. However, it breaks into Zn-bix and RhB in an ethanol–water mixture. The disassembly process is accompanied by fluorescent recovery of released RhB. Thus, the AS of the spirit sample can be quantified by monitoring the fluorescent intensity change of Rhb. In this method, the reported dynamic range is 20% vol to 100% vol.

5. Multi-Responsive MOFs

By the rational design of metal ions and ligands in the complex structure, multi-responsive MOFs can be generated with their optical properties tuned by several stimuli. For example, Wang et al. reported a two dimensional lead (II) based metal–organic framework assembly that is able to tune its luminescent properties upon temperature and nitroaromatic compounds—picric acid [72]. The MOF was composed of 5-aminonicotinic acid as a ligand and Pd (II) as a coordination metal synthesized by the solvothermal method. It exhibits strong broad emission at 496 nm under excitation wavelength at 321 nm in dry state or DMF solution, while it can be quenched significantly in the presence of picric acid (PA). Thus, the as-synthesized materials can be used to detect PA with an LOD of 1.68×10^{-5} mol/L. In addition, it showed good selectivity to PA over other nitroaromatic compounds such as 1,3-dinitrobenzene (1,3-DNB), 2,4-dinitrotoluene (2,4-DNT), nitrobenzene (NB), 4-nitrobenzoic acid (4-NBA) and 1-bromo-4-nitrobenzene (4-BrNB). In terms of the thermoresponsiveness, the luminescent intensity of the coordination complex decreased as the temperature increased from 20 to 300 K, which can be ascribed to thermal activated intramolecular rotation and nonradiative decay at a high temperature. In addition, the luminescent intensity of this complex showed a good linear relationship with temperature in the range of 20 to 150 K with $R^2 = 0.9961$.

Another temperature and pressure dual responsive coordination network was reported by Yao et al., which was composed of $[Cd_3(TPPA)_2(NDA)_3] \cdot (DMF)_{10} \cdot (H_2O)_6$ (TPPA: Tri(4-(pyridine-4-yl)phenyl)amine, NDA: 2,6-naphthalene dicarboxylic acid, DMF: N,N-dimethyl formamide). The coordination complexes can undergo conformation rearrangement and concomitant luminescent property changes upon these stimuli [73]. A pentagonal bipyramidal structure was formed by the coordination between each Cd^{2+} and five carboxylate oxygen atoms (three NDA^{2-}) and two pyridyl nitrogen atoms (two TPPA). The Cd_2 cluster, composed of two Cd^{2+} ions and four carboxyl groups, was squeezed under heat treatment that resulted in a pentagonal bipyramid to octahedron conformational change of Cd^{2+} coordination geometry. The emission color changed from cyan to green with the maximum shifting from 480 nm to 525 nm and with temperature rising from 120 K to 270 K. Upon the pressure applied on the flexible hinged-fence-like scaffold (from 1 atm to 11.12 GPa), the emission color of the crystal showed a gradual shift from green (525 nm) to orange (585 nm), and to red (620 nm) with an intensity decrease. In addition, the deformation of the coordination polymer is reversible once the pressure is removed, with the optical property retained.

The supramolecular assemblies of an organic-decorated chlorobismuthate anion, 1-butyl-2,3-dimethylimidazolium (Bmmim), and a rotationally flexible imidazolium cation, $BiCl_4(2,2'-bipyridine) (bpy), can form two structures as α and β -[Bmmim][$BiCl_4(2,2'$ -bpy)],$

both of which exhibit luminescence properties ascribed to the excited states of metal-to-ligand charge transfer under UV [74]. These luminescent properties can be dynamically tuned on and off through the destruction and re-formation of weak intermolecular interactions upon exposure to ammonia (NH₃) and temperature change. Thus, the greenish-blue emission of α - [Bmmim] [BiCl₄(2,2'-bpy)] and greenish-yellow emission of β assemblies were completely quenched in the presence of NH₃ vapor, while they recovered slowly after the removal of NH₃ at ambient conditions or by heating. Moreover, the β structure can be converted to α state at ambient conditions by the trigger of moisture in the air. Both of these supramolecular assemblies showed high selectivity to NH₃ over other solvents, such as nitrobenzene, toluene, methanol, ethanol, chloroform, dichloromethane, acetonitrile, ethyl acetate, acetone, and diethyl ether, which enhanced the emission.

A triple responsive coordination system was reported by Tripathi et al., in which the photoluminescence of the complex can be dynamically switched by anions, solvent and nitroaromatic compounds [75]. The one-dimensional double chain coordination polymer was synthesized by a benzimidazole-appended tripodal tridentate ligand, 1,3,5-tris(benzimidazolylmethyl)benzene, and Hg²⁺ as metal ions with a formula of $[[\text{Hg}(\text{L})_2] \cdot (\text{ClO}_4)_2]_n$. The weak coordination of ClO₄⁻ ions in the cavity of coordination frameworks allows a complete or partial anion exchange depending upon the incoming anion. The complete anion exchanges were observed in the case of NO₃⁻ and BF₄⁻, while partial exchanges happened with OTf⁻, OTs⁻, and PF₆⁻ anions. In addition, all of the anion-exchanged products showed different degrees of photoluminescent quenching compared to original frameworks, which can be ascribed to various electrostatic/supramolecular interactions (π - π and hydrogen-bonding) of the anions with the framework walls and Hg (II) center, depending upon their size, shape, and coordinating tendencies. The authors also found out that the complexes showed higher affinity toward small anions than larger ones. Furthermore, the fluorescence intensities of coordination complexes are solvent dependent, and the strongest emission was observed in a high hydrolytic environment. In electron-deficient nitro explosives detection in aqueous media, the coordination frameworks showed a fluorescent emission turn off phenomena due to a synergetic effect of electron and energy transfer mechanisms. The Lewis basic pendant bezimidazole moiety, acting as a recognition site, provides good sensitivity of detecting TNP (0.55 ppm) and capability of discriminating nitrophenol (2-, 3- and 4-NP) and nitroaniline (2-NA and 4-NA) isomers efficiently. The authors demonstrated a Hg (II)-based fluorescent coordination polymer that exhibits multi-stimuli responsive behavior for anions, solvents, and nitroaromatic compounds.

6. Summary and Outlook

In this review, we have highlighted recent progress in the field of metal-organic framework-based stimuli-responsive polymers. First, we simply illustrated four types of sensing mechanisms in MOFs in response to different stimuli based on the number of species involved, such as only metal-ligand, metal-ligand-auxiliary ligand, and metal-ligand-guest. Next, physically and chemically responsive MOFs were given in two sections, including temperature, mechanic force, electricity and pH, metal ions, gas, and alcohol responses, respectively. Last, we listed examples of multi-responsive MOFs that are capable of changing properties under two or more stimuli. The diverse combination of ligand-metal chemistry as well as the flexible structure of MOFs makes them ideal candidates for a wide range of applications, such as sensing, targeted drug delivery, wearable electronics, gas storage, etc.

By mastering the design and control of stimuli-responsive behavior, scientists have developed new materials and systems adapted to complex behavior according to external stimuli through a complex chemical network. Most of the system exhibits a linear response to the stimulus that there is one response to one stimulus. However, in nature, one stimulus can lead to a sequence of responses in a non-linear fashion in the signal transduction pathway. It is a challenge for scientists to design more complex systems that are capable of sequential responses similar to the biological signaling cascades. Understanding the

chemical signal transduction mechanisms in the biology system would provide insight into new adaptive materials' design, as well as shed light on the intersection of chemistry, information science, and biology.

In summary, MOF-based stimuli-responsive polymers have been intensively studied and applied in diverse areas due to a myriad of coordination types and their outstanding optical properties. Great potential can be seen in this area, especially if more and more innovative designs of the molecules and interactions can be achieved. If combined with other types of sensing mechanisms and novel designs of stimuli-responsive polymers, MOF-based stimuli-responsive polymers can enormously add merits to sensing technology.

Author Contributions: Writing—original draft preparation, M.W.; writing—review and editing, M.W., Y.W. and X.Z.; funding acquisition, X.Z. All authors have read and agreed to the published version of the manuscript.

Funding: M.W. and X.Z. acknowledge the funding from the National Natural Science Foundation of China (21750110449).

Institutional Review Board Statement: Not applicable.

Informed Consent Statement: Not applicable.

Conflicts of Interest: The authors declare no conflict of interest.

References

1. Chen, J.-K.; Chang, C.-J. Fabrications and applications of stimulus-responsive polymer films and patterns on surfaces: A review. *Materials* **2014**, *7*, 805–875. [[CrossRef](#)] [[PubMed](#)]
2. Hoffman, A.S. “Intelligent” polymers in medicine and biotechnology. *Artif. Organs* **1995**, *19*, 458–467. [[CrossRef](#)] [[PubMed](#)]
3. Wei, M.; Gao, Y.; Li, X.; Serpe, M.J. Stimuli-responsive polymers and their applications. *Polym. Chem.* **2017**, *8*, 127–143. [[CrossRef](#)]
4. Stuart, M.A.C.; Huck, W.T.; Genzer, J.; Müller, M.; Ober, C.; Stamm, M.; Sukhorukov, G.B.; Szleifer, I.; Tsukruk, V.V.; Urban, M. Emerging applications of stimuli-responsive polymer materials. *Nat. Mater.* **2010**, *9*, 101–113. [[CrossRef](#)] [[PubMed](#)]
5. Dong, Y.; Wang, J.; Guo, X.; Yang, S.; Ozen, M.O.; Chen, P.; Liu, X.; Du, W.; Xiao, F.; Demirci, U. Multi-stimuli-responsive programmable biomimetic actuator. *Nat. Commun.* **2019**, *10*, 1–10. [[CrossRef](#)] [[PubMed](#)]
6. Li, G.L.; Tai, C.A.; Neoh, K.; Kang, E.; Yang, X. Hybrid nanorattles of metal core and stimuli-responsive polymer shell for confined catalytic reactions. *Polym. Chem.* **2011**, *2*, 1368–1374. [[CrossRef](#)]
7. Leal, D.A.; Riegel-Vidotti, I.C.; Ferreira, M.G.S.; Marino, C.E.B. Smart coating based on double stimuli-responsive microcapsules containing linseed oil and benzotriazole for active corrosion protection. *Corros. Sci.* **2018**, *130*, 56–63. [[CrossRef](#)]
8. Qiao, Y.; Wan, J.; Zhou, L.; Ma, W.; Yang, Y.; Luo, W.; Yu, Z.; Wang, H. Stimuli-responsive nanotherapeutics for precision drug delivery and cancer therapy. *Wiley Interdiscip. Rev. Nanomed.* **2019**, *11*, e1527. [[CrossRef](#)] [[PubMed](#)]
9. Sood, N.; Bhardwaj, A.; Mehta, S.; Mehta, A. Stimuli-responsive hydrogels in drug delivery and tissue engineering. *Drug Deliv.* **2016**, *23*, 748–770. [[CrossRef](#)] [[PubMed](#)]
10. Conesa-Egea, J.; Zamora, F.; Amo-Ochoa, P. Perspectives of the smart Cu-Iodine coordination polymers: A portage to the world of new nanomaterials and composites. *Coord. Chem. Rev.* **2019**, *381*, 65–78. [[CrossRef](#)]
11. Xie, Z.; Ma, L.; de Krafft, K.E.; Jin, A.; Lin, W. Porous phosphorescent coordination polymers for oxygen sensing. *J. Am. Chem. Soc.* **2009**, *132*, 922–923. [[CrossRef](#)] [[PubMed](#)]
12. Parmar, B.; Rachuri, Y.; Bisht, K.K.; Laiya, R.; Suresh, E. Mechanochemical and conventional synthesis of Zn(II)/Cd(II) luminescent coordination polymers: Dual sensing probe for selective detection of chromate anions and TNP in aqueous phase. *Inorg. Chem.* **2017**, *56*, 2627–2638. [[CrossRef](#)] [[PubMed](#)]
13. Zhang, X.; Wang, W.; Hu, Z.; Wang, G.; Uvdal, K. Coordination polymers for energy transfer: Preparations, properties, sensing applications, and perspectives. *Coord. Chem. Rev.* **2015**, *284*, 206–235. [[CrossRef](#)]
14. Zheng, L.-Y.; Fan, W.-W.; Cheng, Y.; Cao, Q.-E. Reversible Phase Transition of Porous Coordination Polymers. *Chem. Eur. J.* **2020**, *26*, 2766.
15. McConnell, A.J.; Wood, C.S.; Neelakandan, P.P.; Nitschke, J.R. Stimuli-responsive metal–ligand assemblies. *Chem. Rev.* **2015**, *115*, 7729–7793. [[CrossRef](#)] [[PubMed](#)]
16. Deng, J.; Wu, F.; Yu, P.; Mao, L. On-site sensors based on infinite coordination polymer nanoparticles: Recent progress and future challenge. *Appl. Mater. Today* **2018**, *11*, 338–351. [[CrossRef](#)]
17. Higuchi, M. Stimuli-responsive metallo-supramolecular polymer films: Design, synthesis and device fabrication. *J. Mater. Chem. C* **2014**, *2*, 9331–9341. [[CrossRef](#)]
18. Zhang, K.Y.; Liu, S.; Zhao, Q.; Huang, W. Stimuli-responsive metallopolymer. *Coord. Chem. Rev.* **2016**, *319*, 180–195. [[CrossRef](#)]
19. Hu, J.; Liu, S. Engineering responsive polymer building blocks with host–Guest molecular recognition for functional applications. *Acc. Chem. Res.* **2014**, *47*, 2084–2095. [[CrossRef](#)]

20. Yang, Y.; Su, P.; Tang, Y. Stimuli-Responsive Lanthanide-Based Smart Luminescent Materials for Optical Encoding and Bio-applications. *Chemnanomat* **2018**, *4*, 1097–1120. [[CrossRef](#)]
21. Wang, Y.; Pei, Z.; Feng, W.; Pei, Y. Stimuli-responsive supramolecular nano-systems based on pillar [n] arenes and their related applications. *J. Mater. Chem. B* **2019**, *7*, 7656–7675. [[CrossRef](#)]
22. Liu, Z.; Zhang, L.; Sun, D. Stimuli-responsive structural changes in metal–organic frameworks. *Chem. Comm.* **2020**, *56*, 9416–9432. [[CrossRef](#)] [[PubMed](#)]
23. Knebel, A.; Zhou, C.; Huang, A.; Zhang, J.; Kustov, L.; Caro, J. Smart Metal-Organic Frameworks (MOFs): Switching Gas Permeation through MOF Membranes by External Stimuli. *Chem. Eng. Technol.* **2018**, *41*, 224–234. [[CrossRef](#)]
24. Nagarkar, S.S.; Desai, A.V.; Ghosh, S.K. Stimulus-responsive metal–Organic frameworks. *Chem. Asian J.* **2014**, *9*, 2358–2376. [[CrossRef](#)] [[PubMed](#)]
25. Zhang, C.; Che, Y.; Zhang, Z.; Yang, X.; Zang, L. Fluorescent nanoscale zinc (II)-carboxylate coordination polymers for explosive sensing. *Chem. Comm.* **2011**, *47*, 2336–2338. [[CrossRef](#)] [[PubMed](#)]
26. Zeng, H.-H.; Qiu, W.-B.; Zhang, L.; Liang, R.-P.; Qiu, J.-D. Lanthanide coordination polymer nanoparticles as an excellent artificial peroxidase for hydrogen peroxide detection. *Anal. Chem.* **2016**, *88*, 6342–6348. [[CrossRef](#)]
27. Roy, D.; Brooks, W.L.; Sumerlin, B.S. New directions in thermoresponsive polymers. *Chem. Soc. Rev.* **2013**, *42*, 7214–7243. [[CrossRef](#)]
28. Huang, W.; Pan, F.; Liu, Y.; Huang, S.; Li, Y.; Yong, J.; Li, Y.; Kirillov, A.M.; Wu, D. An efficient blue-emissive metal–organic framework (MOF) for lanthanide-encapsulated multicolor and stimuli-responsive luminescence. *Inorg. Chem.* **2017**, *56*, 6362–6370. [[CrossRef](#)]
29. Tom, L.; Kurup, M. A reversible thermo-responsive 2D Zn (II) coordination polymer as a potential self-referenced luminescent thermometer. *J. Mater. Chem. C* **2020**, *8*, 2525–2532. [[CrossRef](#)]
30. Zhang, Y.; Yu, J.; Bomba, H.N.; Zhu, Y.; Gu, Z. Mechanical force-triggered drug delivery. *Chem. Rev.* **2016**, *116*, 12536–12563. [[CrossRef](#)]
31. Di, J.; Yao, S.; Ye, Y.; Cui, Z.; Yu, J.; Ghosh, T.K.; Zhu, Y.; Gu, Z. Stretch-triggered drug delivery from wearable elastomer films containing therapeutic depots. *ACS Nano* **2015**, *9*, 9407–9415. [[CrossRef](#)]
32. Eslahi, N.; Abdorahim, M.; Simchi, A. Smart polymeric hydrogels for cartilage tissue engineering: A review on the chemistry and biological functions. *Biomacromolecules* **2016**, *17*, 3441–3463. [[CrossRef](#)] [[PubMed](#)]
33. Tee, B.C.; Wang, C.; Allen, R.; Bao, Z. An electrically and mechanically self-healing composite with pressure-and flexion-sensitive properties for electronic skin applications. *Nat. Nanotechnol.* **2012**, *7*, 825–832. [[CrossRef](#)] [[PubMed](#)]
34. Li, Q.; Niu, W.; Liu, X.; Chen, Y.; Wu, X.; Wen, X.; Wang, Z.; Zhang, H.; Quan, Z. Pressure-induced phase engineering of gold nanostructures. *J. Am. Chem. Soc.* **2018**, *140*, 15783–15790. [[CrossRef](#)] [[PubMed](#)]
35. Jiang, S.; Luan, Y.; Jang, J.I.; Baikie, T.; Huang, X.; Li, R.; Saouma, F.O.; Wang, Z.; White, T.J.; Fang, J. Phase transitions of formamidinium lead iodide perovskite under pressure. *J. Am. Chem. Soc.* **2018**, *140*, 13952–13957. [[CrossRef](#)] [[PubMed](#)]
36. Rajamanickam, R.; Kwon, K.; Tae, G. Soft and elastic hollow microcapsules embedded silicone elastomer films with enhanced water uptake and permeability for mechanical stimuli responsive drug delivery applications. *Mater. Sci. Eng. C* **2020**, *111*, 110789. [[CrossRef](#)] [[PubMed](#)]
37. Chen, Z.; Tang, J.-H.; Chen, W.; Xu, Y.; Wang, H.; Zhang, Z.; Sepehrpour, H.; Cheng, G.-J.; Li, X.; Wang, P. Temperature-and mechanical-force-responsive self-assembled rhomboidal metallacycle. *Organometallics* **2019**, *38*, 4244–4249. [[CrossRef](#)]
38. Takeda, T.; Ozawa, M.; Akutagawa, T. Jumping Crystal of a Hydrogen-Bonded Organic Framework Induced by the Collective Molecular Motion of a Twisted π System. *Angew. Chem. Int. Ed.* **2019**, *58*, 10345–10352. [[CrossRef](#)]
39. Coudert, F.-X. Responsive metal–organic frameworks and framework materials: Under pressure, taking the heat, in the spotlight, with friends. *Chem. Mater.* **2015**, *27*, 1905–1916. [[CrossRef](#)]
40. Yan, Y.; Chen, J.; Zhang, N.-N.; Wang, M.-S.; Sun, C.; Xing, X.-S.; Li, R.; Xu, J.-G.; Zheng, F.-K.; Guo, G.-C. Grinding size-dependent mechanoresponsive luminescent Cd (II) coordination polymer. *Dalton Trans.* **2016**, *45*, 18074–18078. [[CrossRef](#)] [[PubMed](#)]
41. Đaković, M.; Borovina, M.; PISAČIĆ, M.; Aakeröy, C.B.; Soldin, Ž.; Kukovec, B.M.; Kodrin, I. Mechanically Responsive Crystalline Coordination Polymers with Controllable Elasticity. *Angew. Chem. Int. Ed.* **2018**, *57*, 14801–14805. [[CrossRef](#)]
42. Ramaswamy, P.; Wieme, J.; Alvarez, E.; Vanduyfhuys, L.; Itié, J.-P.; Fabry, P.; Van Speybroeck, V.; Serre, C.; Yot, P.G.; Maurin, G. Mechanical properties of a gallium fumarate metal–organic framework: A joint experimental-modelling exploration. *J. Mater. Chem. A* **2017**, *5*, 11047–11054. [[CrossRef](#)]
43. Yot, P.G.; Yang, K.; Ragon, F.; Dmitriev, V.; Devic, T.; Horcajada, P.; Serre, C.; Maurin, G. Exploration of the mechanical behavior of metal organic frameworks UiO-66 (Zr) and MIL-125 (Ti) and their NH₂ functionalized versions. *Dalton Trans.* **2016**, *45*, 4283–4288. [[CrossRef](#)] [[PubMed](#)]
44. Yot, P.G.; Vanduyfhuys, L.; Alvarez, E.; Rodriguez, J.; Itié, J.-P.; Fabry, P.; Guillou, N.; Devic, T.; Beurroies, I.; Llewellyn, P.L. Mechanical energy storage performance of an aluminum fumarate metal–organic framework. *Chem. Sci.* **2016**, *7*, 446–450. [[CrossRef](#)] [[PubMed](#)]
45. Wu, D.; Li, Y.; Shen, J.; Tong, Z.; Hu, Q.; Li, L.; Yu, G. Supramolecular chemotherapeutic drug constructed from pillararene-based supramolecular amphiphile. *Chem. Comm.* **2018**, *54*, 8198–8201. [[CrossRef](#)] [[PubMed](#)]

46. Kahlfuss, C.; Gibaud, T.; Denis-Quanquin, S.; Chowdhury, S.; Royal, G.; Chevallier, F.; Saint-Aman, E.; Bucher, C. Redox-Induced Molecular Metamorphism Promoting a Sol/Gel Phase Transition in a Viologen-Based Coordination Polymer. *Chem. Eur. J.* **2018**, *24*, 13009–13019. [[CrossRef](#)] [[PubMed](#)]
47. Ni, M.; Zhang, N.; Xia, W.; Wu, X.; Yao, C.; Liu, X.; Hu, X.-Y.; Lin, C.; Wang, L. Dramatically promoted swelling of a hydrogel by pillar [6] arene–ferrocene complexation with multistimuli responsiveness. *J. Am. Chem. Soc.* **2016**, *138*, 6643–6649. [[CrossRef](#)]
48. Fu, S.; Li, F.; Zang, M.; Zhang, Z.; Ji, Y.; Yu, X.; Luo, Q.; Guan, S.; Xu, J.; Liu, J. Diselenium-containing ultrathin polymer nanocapsules for highly efficient targeted drug delivery and combined anticancer effect. *J. Mater. Chem. B* **2019**, *7*, 4927–4932. [[CrossRef](#)]
49. Nakahata, M.; Takashima, Y.; Yamaguchi, H.; Harada, A. Redox-responsive self-healing materials formed from host–guest polymers. *Nat. Commun.* **2011**, *2*, 1–6. [[CrossRef](#)]
50. Xia, W.; Hu, X.-Y.; Chen, Y.; Lin, C.; Wang, L. A novel redox-responsive pillar [6] arene-based inclusion complex with a ferrocenium guest. *Chem. Commun.* **2013**, *49*, 5085–5087. [[CrossRef](#)]
51. Ghoufi, A.; Benhamed, K.; Boukli-Hacene, L.; Maurin, G. Electrically induced breathing of the MIL-53 (Cr) metal–organic framework. *ACS Cent. Sci.* **2017**, *3*, 394–398. [[CrossRef](#)]
52. Fernandez, C.A.; Martin, P.C.; Schaef, T.; Bowden, M.E.; Thallapally, P.K.; Dang, L.; Xu, W.; Chen, X.; McGrail, B.P. An electrically switchable metal–organic framework. *Sci. Rep.* **2014**, *4*, 1–6. [[CrossRef](#)]
53. Mortimer, R.J. Electrochromic materials. *Chem. Soc. Rev.* **1997**, *26*, 147–156. [[CrossRef](#)]
54. Kocak, G.; Tuncer, C.; Bütün, V. pH-Responsive polymers. *Polym. Chem.* **2017**, *8*, 144–176. [[CrossRef](#)]
55. Gao, P.F.; Zheng, L.L.; Liang, L.J.; Yang, X.X.; Li, Y.F.; Huang, C.Z. A new type of pH-responsive coordination polymer sphere as a vehicle for targeted anticancer drug delivery and sustained release. *J. Mater. Chem. B* **2013**, *1*, 3202–3208. [[CrossRef](#)]
56. Ma, K.; Zhao, Y.; Han, X.; Ding, J.; Meng, X.; Hou, H. Interesting pH-responsive behavior in benzothiadiazole-derived coordination polymer constructed via an in situ Click synthesis. *Cryst. Growth Des.* **2018**, *18*, 7419–7425. [[CrossRef](#)]
57. Yan, Q.-Q.; Li, B.; Jiang, W.-P.; Xu, Y.-B.; Xu, Z.-Q.; Yong, G.-P. Reversible stimulus-responsive coordination polymers mainly involving conversion between the lone-pair– π and cation– π interactions. *J. Coord. Chem.* **2020**, *73*, 854–866. [[CrossRef](#)]
58. Tan, L.; Fan, T.; Xia, T.; Cui, Y.; Yang, Y.; Qian, G. A luminescent terbium metal–organic framework for highly sensitive and selective detection of uric acid in aqueous media. *J. Solid State Chem.* **2019**, *272*, 55–61. [[CrossRef](#)]
59. Faulkner, S.; Pope, S.J. Lanthanide-sensitized lanthanide luminescence: Terbium-sensitized ytterbium luminescence in a trinuclear complex. *J. Am. Chem. Soc.* **2003**, *125*, 10526–10527. [[CrossRef](#)] [[PubMed](#)]
60. Sabbatini, N.; Guardigli, M.; Lehn, J.-M. Luminescent lanthanide complexes as photochemical supramolecular devices. *Coord. Chem. Rev.* **1993**, *123*, 201–228. [[CrossRef](#)]
61. Shi, X.; Qu, X.; Chai, J.; Tong, C.; Fan, Y.; Wang, L. Stable coordination polymers with linear dependence color tuning and luminescent properties for detection of metal ions and explosives. *Dye. Pigment.* **2019**, *170*, 107583. [[CrossRef](#)]
62. Guan, X.-W.; Lin, Q.; Zhang, Y.-M.; Wei, T.-B.; Wang, J.; Fan, Y.-Q.; Yao, H. Pillar [5] arene-based spongy supramolecular polymer gel and its properties in multi-responsiveness, dye sorption, ultrasensitive detection and separation of Fe^{3+} . *Soft Matter* **2019**, *15*, 3241–3247. [[CrossRef](#)] [[PubMed](#)]
63. Kumpfer, J.R.; Jin, J.; Rowan, S.J. Stimuli-responsive europium-containing metallo-supramolecular polymers. *J. Mater. Chem.* **2010**, *20*, 145–151. [[CrossRef](#)]
64. Knapton, D.; Burnworth, M.; Rowan, S.J.; Weder, C. Fluorescent Organometallic Sensors for the Detection of Chemical-Warfare-Agent Mimics. *Angew. Chem. Int. Ed.* **2006**, *45*, 5825–5829. [[CrossRef](#)] [[PubMed](#)]
65. Li, J.-R.; Kuppler, R.J.; Zhou, H.-C. Selective gas adsorption and separation in metal–organic frameworks. *Chem. Soc. Rev.* **2009**, *38*, 1477–1504. [[CrossRef](#)] [[PubMed](#)]
66. Chen, C.; Rao, H.; Lin, S.; Zhang, J. A vapochromic strategy for ammonia sensing based on a bipyridinium constructed porous framework. *Dalton Trans.* **2018**, *47*, 8204–8208. [[CrossRef](#)]
67. Yanai, N.; Kitayama, K.; Hijikata, Y.; Sato, H.; Matsuda, R.; Kubota, Y.; Takata, M.; Mizuno, M.; Uemura, T.; Kitagawa, S. Gas detection by structural variations of fluorescent guest molecules in a flexible porous coordination polymer. *Nat. Mater.* **2011**, *10*, 787–793. [[CrossRef](#)]
68. Xia, D.; Ma, J.; Wang, P. A hydrogen sulfide-sensitive supramolecular polymer constructed by crown ether-based host–Guest interaction and Ag-coordination. *Sens. Actuators B Chem.* **2019**, *279*, 197–203. [[CrossRef](#)]
69. Coronado, E.; Giménez-Marqués, M.; Espallargas, G.M.; Brammer, L. Tuning the magneto-structural properties of non-porous coordination polymers by HCl chemisorption. *Nat. Commun.* **2012**, *3*, 1–8. [[CrossRef](#)]
70. Deng, J.; Shi, G.; Zhou, T. Colorimetric assay for on-the-spot alcoholic strength sensing in spirit samples based on dual-responsive lanthanide coordination polymer particles with ratiometric fluorescence. *Anal. Chim. Acta* **2016**, *942*, 96–103. [[CrossRef](#)]
71. Deng, J.; Ma, W.; Yu, P.; Mao, L. Colorimetric and fluorescent dual mode sensing of alcoholic strength in spirit samples with stimuli-responsive infinite coordination polymers. *Anal. Chem.* **2015**, *87*, 6958–6965. [[CrossRef](#)]
72. Wang, L. A Dual-Functional Lead (II) Metal–Organic Framework Based on 5-Aminonicotinic Acid as a Luminescent Sensor for Selective Sensing of Nitroaromatic Compounds and Detecting the Temperature. *J. Inorg. Organomet. Polym. Mater.* **2020**, *30*, 291–298. [[CrossRef](#)]
73. Yao, Z.Q.; Xu, J.; Zou, B.; Hu, Z.; Wang, K.; Yuan, Y.J.; Chen, Y.P.; Feng, R.; Xiong, J.B.; Hao, J. A Dual-Stimuli-Responsive Coordination Network Featuring Reversible Wide-Range Luminescence-Tuning Behavior. *Angew. Chem. Int. Ed.* **2019**, *58*, 5614–5618. [[CrossRef](#)] [[PubMed](#)]

-
74. Shen, N.; Li, J.; Li, G.; Hu, B.; Li, J.; Liu, T.; Gong, L.; Huang, F.; Wang, Z.; Huang, X. Designing Polymorphic Bi³⁺-Containing Ionic Liquids for Stimuli-Responsive Luminescent Materials. *Inorg. Chem.* **2019**, *58*, 8079–8085. [[CrossRef](#)] [[PubMed](#)]
 75. Tripathi, S.; Bardhan, D.; Chand, D.K. Multistimuli-responsive hydrolytically stable “smart” mercury (II) coordination polymer. *Inorg. Chem.* **2018**, *57*, 11369–11381. [[CrossRef](#)] [[PubMed](#)]